



# Tsunamigenic predecessors to the 2009 Samoa earthquake

Emile A. Okal<sup>a,\*</sup>, José C. Borrero<sup>b,c</sup>, Catherine Chagué-Goff<sup>d,e</sup>

<sup>a</sup> Department of Earth & Planetary Sciences, Northwestern University, Evanston, IL 60201, USA

<sup>b</sup> Department of Civil Engineering, University of Southern California, Los Angeles, CA 90089, USA

<sup>c</sup> ASR Ltd., 1 Wainui Road, Raglan 3225, New Zealand

<sup>d</sup> Natural Hazards Research Lab and Australian Tsunami Research Centre, School of Biological, Earth and Environmental Sciences, University of New South Wales, Sydney 2052, NSW, Australia

<sup>e</sup> Institute for Environmental Research, Australian Nuclear Science and Technology Organisation, Locked Bag 2001, Kirrawee DC, NSW 2232, Australia

## ARTICLE INFO

### Article history:

Received 14 July 2010

Accepted 29 December 2010

Available online 13 January 2011

### Keywords:

tsunami

Samoa

Historical earthquakes

## ABSTRACT

We analyze historical earthquakes of the past century having generated regional tsunamis in Samoa, by means of epicentral relocation and quantification of spectral amplitudes of waveforms from historical seismograms. The only tsunami with a level of destruction comparable to the 2009 event was generated by the earthquake of 26 June 1917 in the Samoa corner. Yet, a memory of this event is largely absent from the ancestral heritage of the present population of Samoa, which we tentatively attribute to the nearly simultaneous occurrence of the influenza epidemic in 1918. While not able to fully resolve focal geometries, we document a diversity of mechanisms, which add an element of unpredictability to the forecast of any future tsunami in the region.

© 2010 Published by Elsevier B.V.

## Contents

1. Introduction . . . . .	128
2. Methodology . . . . .	129
2.1. Relocations . . . . .	129
2.2. Focal solutions . . . . .	129
2.3. Tsunami simulations . . . . .	130
3. 01 September 1981 . . . . .	131
4. 26 December 1975 . . . . .	131
5. 08 September 1948 . . . . .	132
6. The 1917 and 1919 earthquakes . . . . .	133
6.1. The 1917 and 1919 tsunamis . . . . .	133
6.2. Seismological study: Event I, 01 May 1917 . . . . .	136
6.3. Seismological study: Event II, 26 June 1917 . . . . .	136
6.4. Seismological study: Event III, 01 January 1919 . . . . .	137
6.5. Seismological study: Event IV, 30 April 1919 . . . . .	137
7. Other notable events . . . . .	138
8. Conclusion . . . . .	138
Acknowledgments . . . . .	139
References . . . . .	139

## 1. Introduction

The purpose of this paper is to conduct a study of predecessors to the 2009 Samoa earthquake. This major event ( $M_0 = 1.8 \times 10^{28}$  dyn cm) generated the first tsunami in 45 years to create

significant damage and casualties on U.S. soil, which was also the most devastating one in at least 92 years in the South Pacific West of the South American subduction zone.

The 2009 earthquake featured normal faulting in the outer rise of the curving subduction interface, in a complex geometry defined as a STEP (“Subduction-Transform Edge Propagator”) by [Govers and Wortel \(2005\)](#). Its source was itself complex, featuring a strong non-double-couple component ( $\epsilon = 0.15$  to  $0.30$ ) as a result of the

\* Corresponding author.

E-mail address: [emile@earth.northwestern.edu](mailto:emile@earth.northwestern.edu) (E.A. Okal).

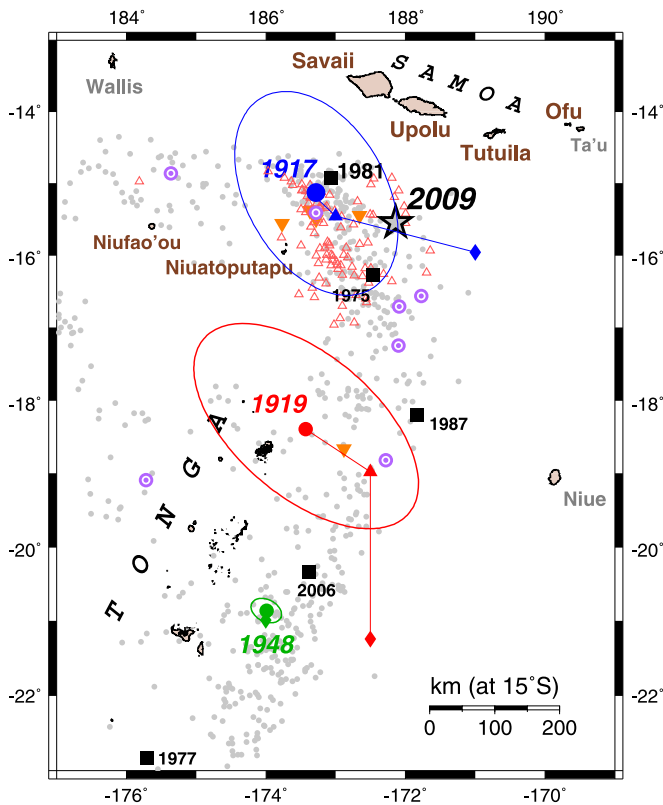


**Fig. 1.** Location map of the study area. The boundary of the Pacific plate is defined by the database of CMT solutions shallower than 50 km (small gray dots); those with a moment greater than  $10^{26}$  dyn cm are shown as bull's eye symbols. The large earthquakes of 26 June 1917, 30 April 1919 and 08 September 1948, relocated using the algorithm of Wyssession et al. (1991), are shown as solid dots (with confidence ellipses); the triangles are Gutenberg and Richter's (1954) epicenters, and the diamonds the ISS solutions. The 2009 Samoa earthquake is shown as the gray star. Other earthquakes with decimetric tsunamis in Samoa are shown as black squares; the inverted triangles are relocated epicenters of other events North of 20°S, predating 1963, with at least one magnitude  $>7$  and without tsunami reports. The small red open triangles are earthquakes occurring during a 24-h window following the mainshock of 29 September 2009. Adapted from Okal et al. (2004) and Okal et al. (2010).

triggering of coseismic slip on the subduction interface following the outer rise rupture, a model proposed by Li et al. (2009) and later refined by Lay et al. (2010). As difficult as the concept of recurrence times may be for regular subduction events, we know even less about the repeat patterns of outer rise events, except that they are usually thought to feature much longer cycles (Kirby et al., 2008).

**Table 1**

Parameters of seismic events relocated in this study.

Date D M (J) Y	Origin time (GMT)	Latitude (°N)	Longitude (°E)	Depth (km)	Number of stations		R.M.S. $\sigma$ (s)
					Available	Used	
01 MAY (121) 1917	18:26:40.0	-29.39	-179.29	10.0	20	12	7.75
26 JUN (177) 1917	5:49:40.8	-15.13	-173.28	10.0	28	22	7.55
16 NOV (320) 1917	3:19:36.8	-28.67	-178.42	10.0	19	15	6.34
01 JAN (001) 1919	3:00:11.3	-19.52	-177.61	246.4f	21	13	3.30
30 APR (120) 1919	7:17:16.6	-18.48	-173.35	20.0	24	21	5.32
27 FEB (058) 1921	18:23:35.7	-18.60	-172.99	10.0	30	27	3.84
08 JUN (159) 1939	20:46:54.8	-15.56	-173.77	86.5f	62	60	2.88
29 JUN (181) 1948	10:28:34.0	-15.45	-172.66	15.0	81	79	3.06
08 SEP (252) 1948	15:09:11.9	-20.89	-173.94	10.0	76	72	3.18
18 APR (108) 1949	21:34:45.7	-15.50	-173.28	35.9f	33	33	1.76
27 NOV (331) 1949	8:42:15.0	-17.69	-173.23	7.8f	59	56	2.71
14 APR (104) 1957	19:18:00.0	-15.38	-173.37	10.0	166	165	2.90

f: floated depth; all others constrained during relocation.

In this context, it is worth examining in detail the historical seismicity of the Samoa corner; we focus in this paper on those events in the 20th century that were large enough to generate observable or locally damaging tsunamis, and for which instrumental seismic data is available. The record of tsunamis in the Tonga–Samoa area was compiled as part of Solov'ev and Go's (1975, translated in 1984) monumental and authoritative monograph, based on various original reports, and augmented by its complement for the years 1969–1982 (Solov'ev et al., 1986). Later, Pararas-Carayannis and Dong (1980) complemented their analysis by researching newspaper accounts of the events reported by the individual chronicles compiled by Solov'ev and Go (1975).

## 2. Methodology

For each of the events considered (Fig. 1), we present a general description, including the effects of the tsunami, as compiled from various literature sources. We then conduct a seismological study combining the following approaches:

### 2.1. Relocations

For events predating the dawn of modern seismology (1963), we use the techniques of Wyssession et al. (1991) to relocate the earthquake sources based on arrival times published by the International Seismological Summary (ISS). This interactive iterative least-squares method uses a Monte Carlo algorithm to inject Gaussian noise into the dataset in order to define a confidence ellipse for the relocated epicenter; the standard deviation of the noise varies from  $\sigma_G = 1$  s for modern events (ca. 1963) to  $\sigma_G = 15$  s in the 1910s. We take the present opportunity to relocate not only the targeted tsunamigenic earthquakes, but also other major events in the area. Our relocation results are given in Table 1. Incidentally, we note that only one of the events studied here (01 January 1919) was relocated by Engdahl and Villaseñor (2002).

### 2.2. Focal solutions

For earthquakes postdating 1976, these are available from the CMT catalogue (Dziewonski et al., 1981 and subsequent quarterly updates). For the period 1963–1975, we use WWSSN analog data, permanently archived at Northwestern University, to build focal solutions based on first motion *P*-wave data, and obtain long-period seismic moments from the analysis of spectral amplitudes of selected mantle waves recorded at high-quality long-period stations. For historical earthquakes predating 1963, we have found it generally impossible in the present cases to use the PDFM algorithm introduced by Reymond and Okal (2000), and which consists of inverting only

**Table 2**  
Seismic moments obtained or used in the present study.

Date	Reference	Seismic moment		
		( $10^{28}$ dyn cm)	Reference	Method
17 NOV 1865		4	a	Far-field tsunami
01 MAY 1917	Event I	2.3	b	$M_c$
26 JUN 1917	Event II	1.2	b	$M_m$
01 JAN 1919	Event III	0.6	b	$M_c$
30 APR 1919	Event IV	1.1	b	$M_c$
08 SEP 1948		0.25	b	$M_c$
26 DEC 1975		0.3	b	$M_c$
01 SEP 1981		0.19	c	CMT
29 SEP 2009		1.8	d	CMT

a: Okal et al. (2004).

b: This study.

c: Dziewonski et al. (1988).

d: average of preliminary determinations; see Okal et al. (2010) for details.

the spectral amplitude of mantle Love and Rayleigh waves (while discarding the phase information). This is due to the general scarcity

of the available datasets of mantle waveforms, and especially to their repartition in azimuth, most records available to us coming from Europe. Rather, we estimate long-period moments based on mantle magnitude measurements (Okal and Talandier, 1989), occasionally corrected for a focal mechanism estimated or inspired by neighboring modern (and generally smaller) events, and constrained by occasional body-wave data. Table 2 regroups the moments obtained or used in this study.

### 2.3. Tsunami simulations

Once an estimate of the geometry and moment of an event has been obtained, we use scaling laws (Geller, 1976) to derive a model of the rupture parameters of the earthquake, which are then taken as initial conditions of a numerical simulation of the tsunami in the area of the Samoa Islands, using the MOST code (Titov and Synolakis, 1998), which solves the non-linear equations of hydrodynamics under the shallow water approximation, using the method of alternating steps, over a number of nested grids. The regional computation is carried out on a 1.5-minute grid (2.75 km), and a

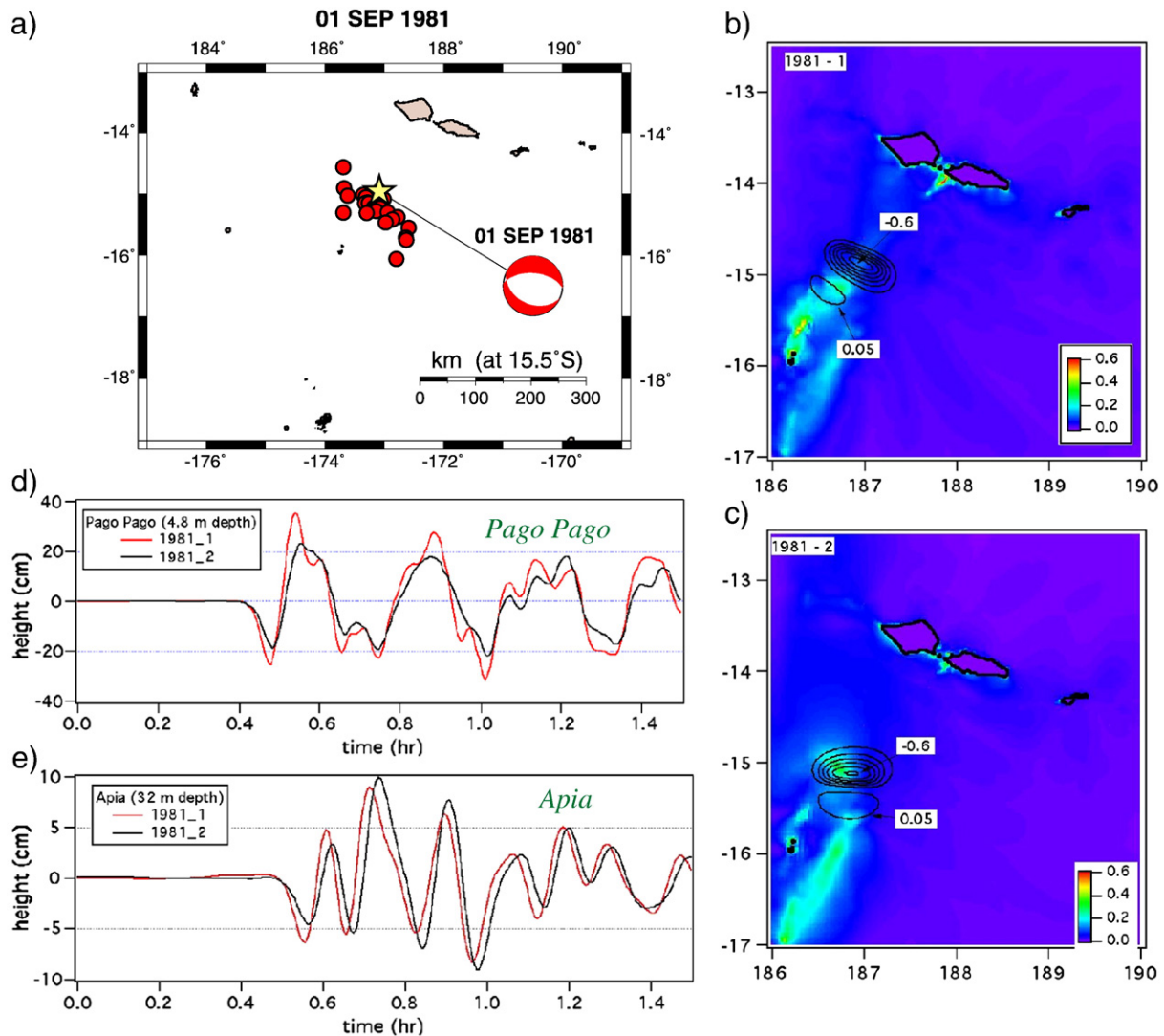


**Fig. 2.** (a): Location (star) and CMT solution of the earthquake of 01 September 1981. The solid dots are the 2-month aftershocks located by the NEIC. (b): Simulation of the 1981 tsunami for the preferred mechanism ( $\phi = 115^\circ$ ,  $\delta = 37^\circ$ ,  $\lambda = -73^\circ$ ). The solid lines contour the field of static displacement (in m), ranging from an uplift of 5 cm to the Southwest to a subsidence of 60 cm to the Northeast. The field of maximum displacement of sea surface for a duration of 1.5 hour following the event is color-coded according to the bar at right (in meters). (c): Same as (b) for the conjugate mechanism ( $\phi = 274^\circ$ ,  $\delta = 55^\circ$ ,  $\lambda = -102^\circ$ ). (d): Simulation time series of the tsunami at the entrance to the harbor of Pago Pago for the preferred model (red trace) and the conjugate one (black trace). (e): Same as (d) for Apia. Note the minor differences between the two.

local computation for Apia and Pago Pago harbors uses a refined grid digitized at a spacing of 0.1 arc-minute (~180 m).

We examine the main events in order of increasing age.

### 3. 01 September 1981

This earthquake took place at 14.96°S, 173.09°W, 130 km to the WNW of the 2009 epicenter (Fig. 2). The effects of its tsunami are described in Solov'ev et al. (1986), who report that it inundated the village of Taga on Savai'i with wave heights reported at 1 m, but resulted in no casualties on any of the islands. However, since the village is built on a bluff, and was not flooded in 2009, it is probable that this report relates to the few houses and fishing infrastructure located along the coastal road (H. Fritz, pers. comm., 2010). The maregraph at Apia recorded a maximum amplitude of 10 cm.

The CMT mechanism of the earthquake,  $\phi = 115^\circ$ ,  $\delta = 37^\circ$ ,  $\lambda = -73^\circ$  (Dziewonski et al., 1988), is rotated 57° from that of 2009, in the formalism of Kagan (1991). The distribution of aftershocks favors the southwards dipping plane, along which the mechanism expresses the tear of the Pacific plate, whose Southern part subducts under the

Lau Basin, while the Northern block continues its motion parallel to the Samoa chain.

The seismic moment is given as  $M_0 = 1.94 \times 10^{27}$  dyn cm, which makes the event about 10 times smaller than the 2009 one. Based on scaling laws (Geller, 1976), we assume a fault length  $L = 64$  km, a fault width  $W = 32$  km, and a slip  $\Delta u = 1.9$  m. We conduct simulations for both focal models, with results shown on Fig. 2b–d. Note that they correctly predict maximum amplitudes on the Southwestern shores of Upolu and in the straits separating it from Savai'i. The maximum amplitude recorded at Apia (10 cm) is correctly modeled by either model.

### 4. 26 December 1975

This earthquake took place at 16.27°S, 172.47°W, just 97 km SSW of the 2009 epicenter (Fig. 3a). It generated only a minor tsunami, which was measured at 15 cm in Apia and reported at 75 cm in Pago Pago by Solov'ev et al. (1986). By contrast, the NOAA tsunami database reports only 38 cm at Pago Pago, which suggests that Solov'ev et al.'s (1986) figure may be a peak-to-peak value.

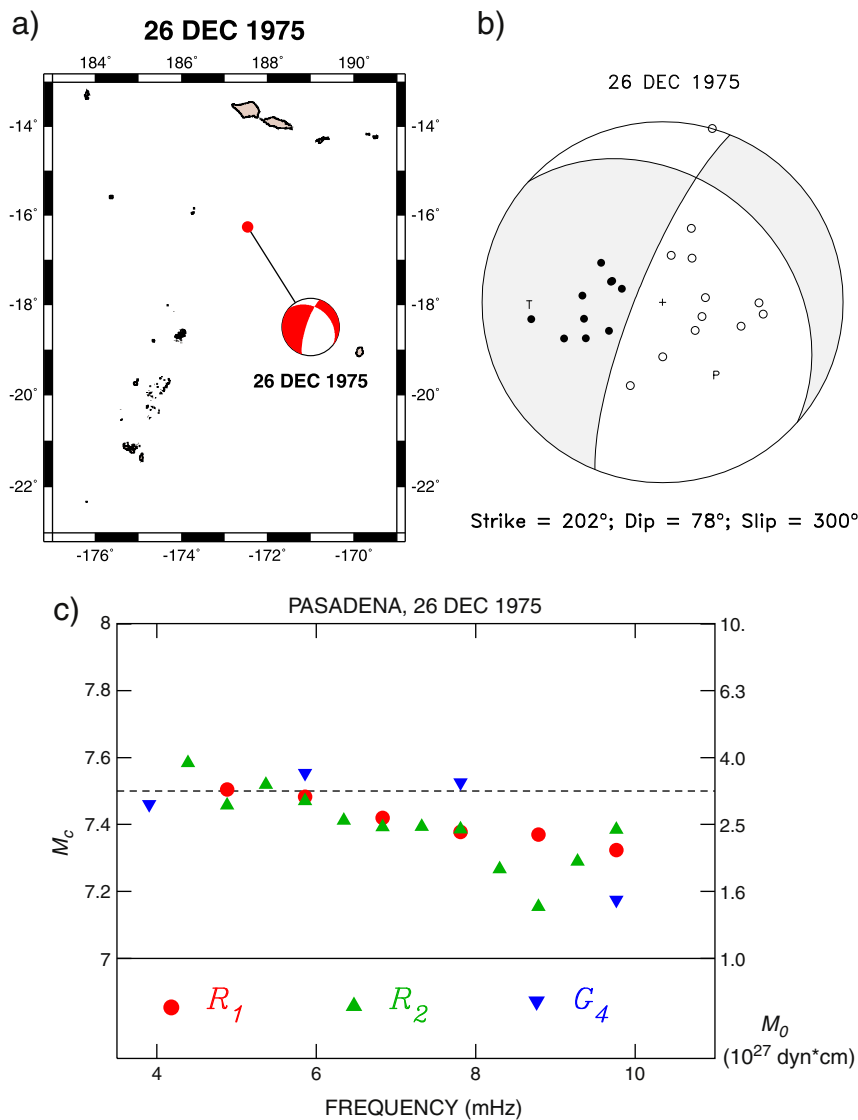


**Fig. 3.** (a): Location of the 1975 earthquake. (b): Focal mechanism compiled from firstmotion P-wave polarities; (c): Spectral amplitudes of mantle waves recorded at Pasadena, interpreted as magnitudes  $M_c$  (Okal and Talandier, 1989) corrected for the focal mechanism obtained in (b). The dashed line represents the inferred static value of the moment used in the hydrodynamic simulation.



We present on Fig. 3b a focal mechanism compiled from  $P$ -wave first motions read at WWSSN and other stations. The mechanism ( $\phi = 202^\circ$ ;  $\delta = 78^\circ$ ;  $\lambda = 300^\circ$ ) is well constrained and features nearly pure dip-slip on a steeply dipping plane striking SSW, while the conjugate mechanism ( $\phi = 312^\circ$ ;  $\delta = 32^\circ$ ;  $\lambda = 203^\circ$ ) represents a right-lateral strike-slip motion on a plane dipping shallowly to the NNE.

Mantle surface waves were superbly recorded at Pasadena, notably on the ultra-long period “33” Benioff instrument (Fig. 4). We use 1st and 2nd passages of Rayleigh waves, and a fourth passage of Love waves recorded on the Press–Ewing instrument, to recover spectral amplitudes in the range 4–10 mHz. When corrected for the above focal mechanism, they yield mantle magnitudes  $M_c$  (Okal and Talandier (1989) which can be directly interpreted in terms of seismic moments. Fig. 3c suggests a static value of  $3 \times 10^{27}$  dyn cm, which in turn yields source parameters  $L = 75$  km,  $W = 37$  km, and  $\Delta u = 2.2$  m.

We present on Fig. 5 the results of our simulations for both focal mechanisms. Both match the value reported at Pago Pago by the NOAA database (but fall short of Solov'ev et al.'s (1986) report), but only the second mechanism reproduces the amplitude reported at Apia. In addition, the first mechanism predicts a strong focusing at Niuatoputapu and Tafahi, where deep-water amplitudes reaching 60 cm should have led to metric amplitudes on the islands, which in turn should

have been observed, whereas none of the witnesses interviewed during our 2009 survey (Okal et al., 2010) remembered a tsunami in 1975. For these reasons, we prefer the conjugate mechanism. Note that the distribution of aftershocks cannot resolve the focal solution.

### 5. 08 September 1948

This earthquake was relocated as part of Okal et al.'s (2004) study at  $20.89^\circ\text{S}$ ,  $173.94^\circ\text{W}$ , off the Ha'apai group of the Tonga Islands (Fig. 6a). It generated a moderate tsunami, recorded with 10-cm amplitudes at Pago Pago, but without documented reports of direct observations or damage in the Samoa Islands (Pararas-Carayannis and Dong, 1980; Solov'ev and Go, 1984).

Excellent records of this event are available at Pasadena and Tucson, featuring sharp negative  $P$ -wave first motions, and a strong  $S$  wave impulsive to the North (Fig. 6). These polarities rule out an interplate thrust mechanism, and suggest that the 1948 earthquake may be comparable to the large event of 22 June 1977 (Talandier and Okal, 1979; Lundgren and Okal, 1988), a normal faulting earthquake expressing a break in the downgoing slab, 300 km to the SSW. Additional first motions reported in the ISS (anaseismic at Riverview and for  $PKP$  in Europe) are also compatible with this interpretation. Assuming that the two events share a common focal geometry ( $\phi = 14^\circ$ ;  $\delta = 11^\circ$ ;  $\lambda = -93^\circ$ ), we use the mantle wave records at Pasadena

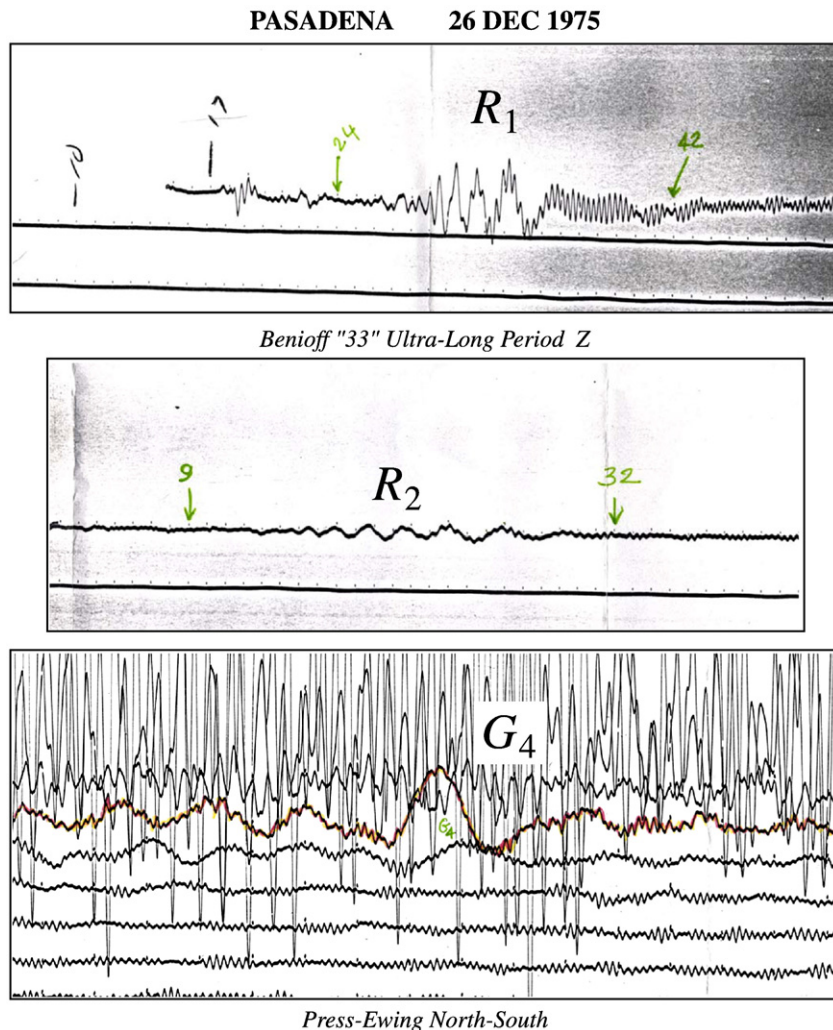


**Fig. 4.** Long-period records of mantle surface waves obtained at Pasadena for the Samoa event of 26 December 1975. *Top and center:* First and second passages of Rayleigh waves on the ultra-long period “33” instrument. Ticks are minute marks; hand-written figures specify minutes bracketing windows used in  $M_c$  calculations. *Bottom:* Fourth passage of the Love wave on Press–Ewing North–South instrument. Ticks are minute marks.

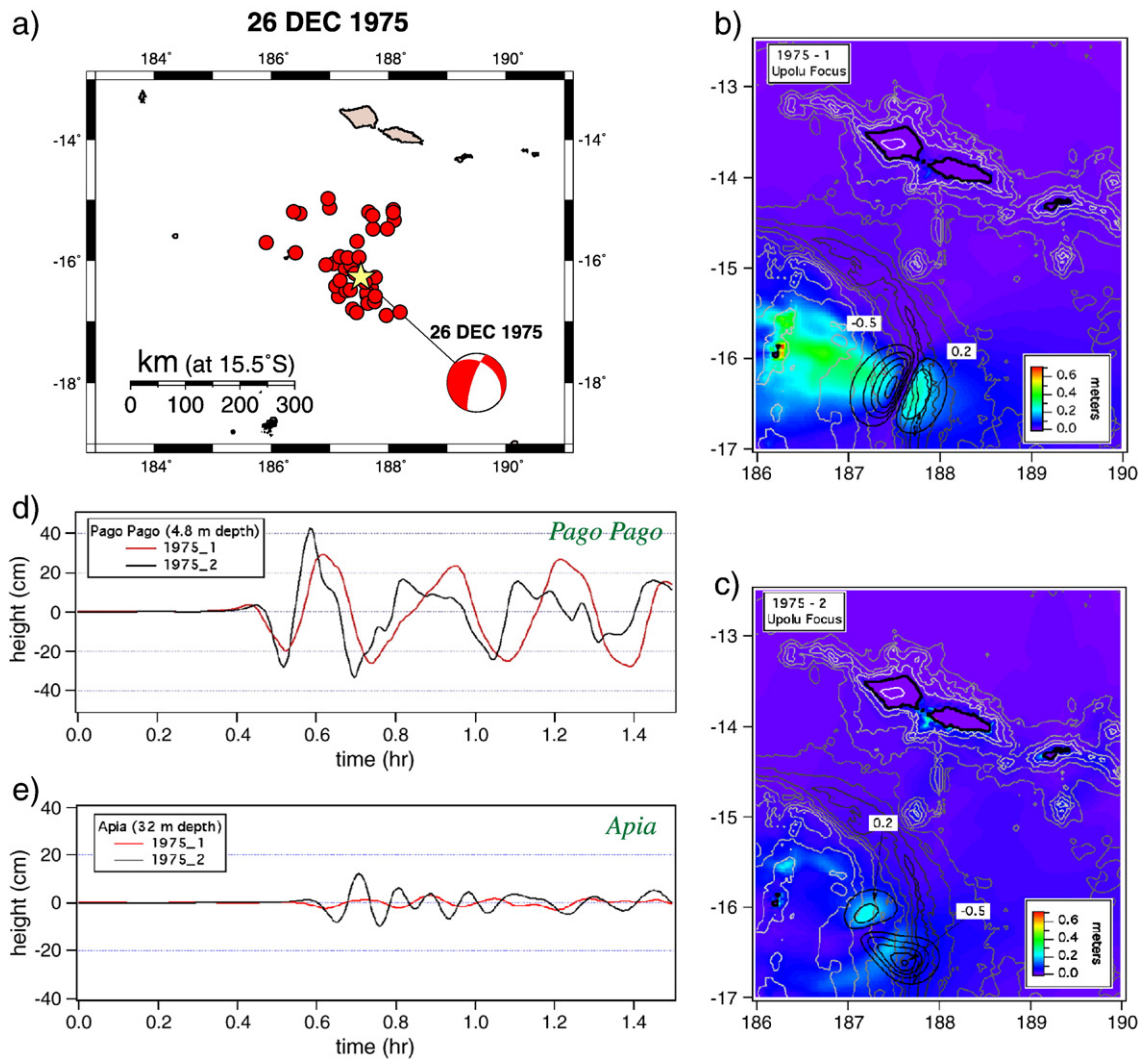


**Fig. 5.** Same as Fig. 2 for the event of 26 December 1975. Frame (b) and the red traces use the steeply dipping fault plane ( $\phi = 115^\circ$ ,  $\delta = 37^\circ$ ,  $\lambda = -73^\circ$ ); Frame (c) and the black traces use the shallow one ( $\phi = 312^\circ$ ;  $\delta = 32^\circ$ ;  $\lambda = 203^\circ$ ), which is preferred. Note that the 2-month aftershocks fail to resolve the fault plane.

( $R_1$ ,  $G_1$ ,  $G_2$ ) to infer an average moment of  $2.5 \times 10^{27}$  dyn cm (Fig. 6e). This moderate earthquake size explains the lack of an observable tsunami in Samoa, at a distance of 750 km, and thus does not warrant numerical simulation.

## 6. The 1917 and 1919 earthquakes

Over a period of two years, the Kermadec–Tonga–Samoa subduction system was the site of four major events (Fig. 7), all with “Pasadena magnitudes”  $M_{PAS} \geq 8.3$ , as later assigned by Gutenberg and Richter (1954).

On 01 May 1917, Event I struck the Kermadec Islands, with  $M_{PAS} = 8.6$ . It was soon followed by an earthquake in Samoa (Event II; 26 June 1917;  $M_{PAS} = 8.7$ ), then 18 months later by an event in Tonga (Event III; 01 Jan 1919;  $M_{PAS} = 8.3$ ; listed at a depth of 180 km by Gutenberg and Richter (1954)), and finally 4 months later by another Tongan earthquake (Event IV; 30 Apr 1919;  $M_{PAS} = 8.4$ ). As will be discussed in detail, these four events have large but non-intersecting confidence ellipses, and there can be no doubt that they occurred in different geographic provinces.

A considerable amount of confusion exists concerning these earthquakes, and in particular the effects of their tsunamis. This is due to the proximity of the relevant dates (a mere 56 days separate the two 1917 shocks and 119 days the events of 1919).

### 6.1. The 1917 and 1919 tsunamis

Following Event I in the Kermadec Islands, Heck (1947) reports a large tsunami with waves reaching 12 m “at Samoa” (without further specifying the location), and recorded on maregraphs in North America. This considerable amplitude at a distance of 1800 km is intriguing, and Iida et al. (1967) suggested that this report results from confusion with Event II’s tsunami, occurring 56 days later. Heck’s (1947) primary reference is the ISS, which could not be confirmed by Paras-Carayannis and Dong (1980), who did not have access to the relevant issue of the ISS. The latter, available at Northwestern University, makes no mention of a tsunami generated by any of Events I–IV, which renders Heck’s (1947) report questionable. Angenheister (1920) lists tsunami arrival times in Honolulu and North America, but not at Apia, where the arrival of the wave coincided with a change of record.

The tsunami generated by Event II (26 June 1917) is described by Solov’ev and Go (1975, 1984) who transcribe Heck’s (1947) report of 12-m (40-ft) waves, itself referenced to an anonymous entry to the First Pacific Science Congress, while Angenheister (1920) publishes the Apia maregram (reproduced on Fig. 8a), documenting a peak-to-peak amplitude of no more than 90 cm (vs. 70 cm zero-to-peak in 2009). Paras-Carayannis and Dong (1980) quote excerpts from local newspapers describing a devastating tsunami, especially on the Southeastern coast of Upolu (Lotofaga), and to a lesser extent in Pago Pago. While

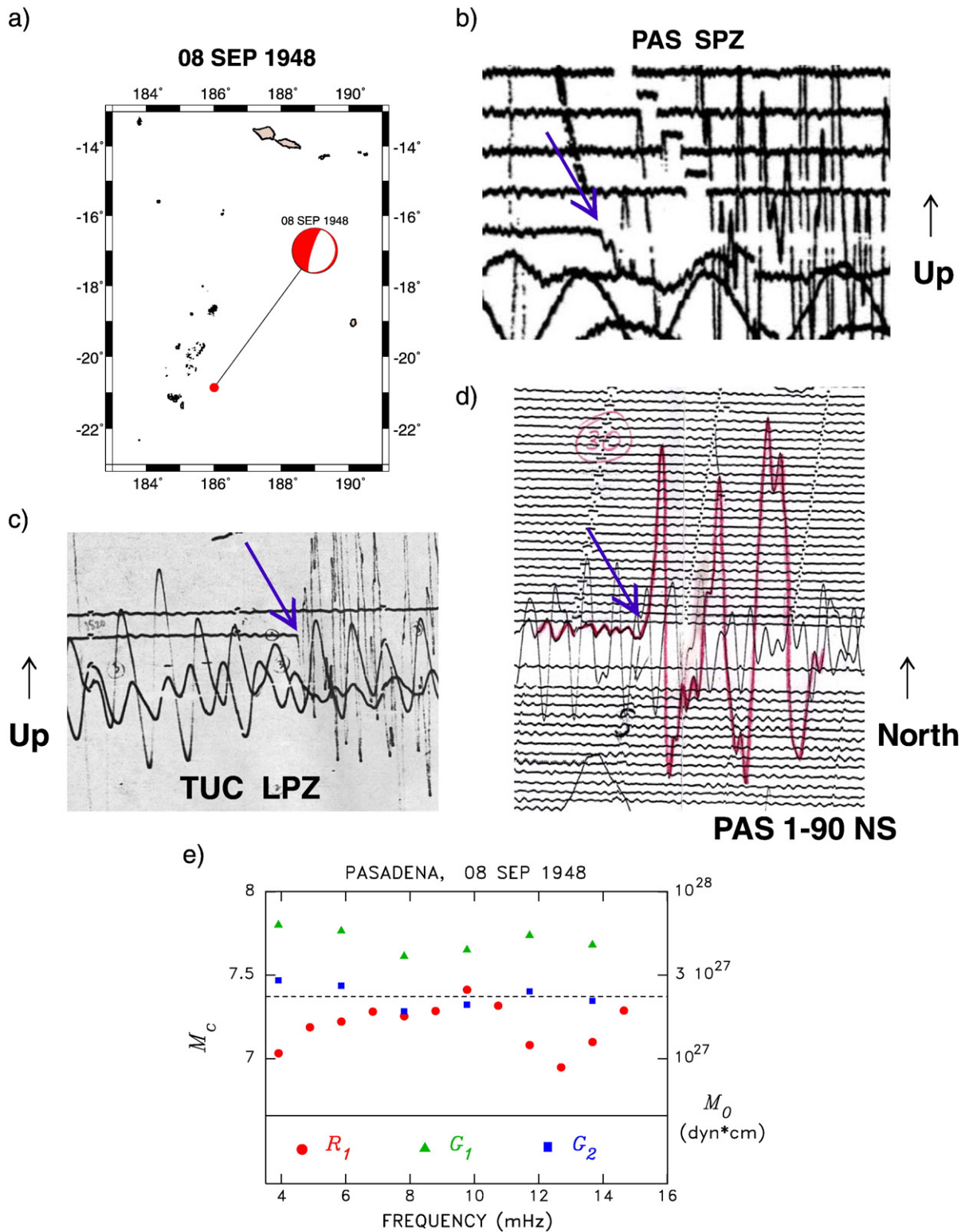


**Fig. 6.** Study of the Tonga event of 08 September 1948. (a) Location and proposed mechanism. (b, c, d): Examples of body-wave polarities (P at PAS and TUC; S at PAS) used to estimate focal mechanism. (e) Estimation of moment from spectral amplitudes at Pasadena (see Fig. 3c for details).

these descriptions are difficult to quantify, they suggest flow depths at Lotofaga of about 3 m, which again would be smaller than in 2009.

Solov'ev and Go (1984) report that the tsunami arrived in Honolulu with a period of 20 minutes, 7.7 hours after the earthquake. This would correspond to a very slow group velocity of 157 m/s, which under the shallow-water approximation, would require an average ocean depth of no more than 2500 m. Rather, we surmise that

this observation could correspond to much shorter waves (with a period of around 3 mn), dispersed outside the SWA, but aliased by the strongly non-linear nature of the maregraph. Delayed arrivals subject to amplification inside distant harbors have been reported in Madagascar, Réunion and Tanzania following the 2004 Sumatra tsunami, and more recently in the Marquesas following the Maule, Chile tsunami (Okal et al., 2006a,b, 2009; Reymond et al., 2010). An



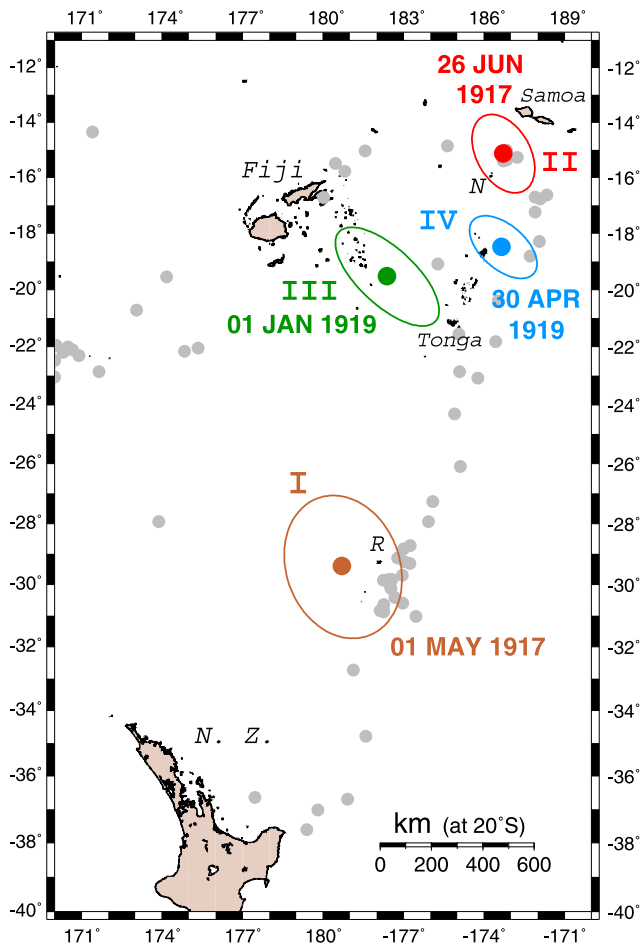


**Fig. 7.** Relocation of the four large events of 1917–1919. For each of them, we show the relocated epicenter and its Monte Carlo ellipse, computed for  $\sigma_c = 15$  s. The islands of Raoul (R) and Niuatoputapu (N), mentioned in the text, are identified.

alternative explanation would involve wave trapping and resonance in the shallow bathymetry surrounding the Hawaiian chain.

Regarding Event III, there are no documented reports of a local tsunami, but [Imamura and Moriya \(1939\)](#) mention a tsunami recorded with an amplitude of 40 cm in Japan, which they attribute to Event III. This association is however disputed by [Iida et al., \(1967\)](#) on the basis of the absence of more local reports, and of misfits in both absolute and relative arrival times.

Finally, Event IV generated a tsunami well documented in Tonga ([Angenheister, 1920](#)) with wave heights on the order of 2.5 m ([Solov'ev and Go, 1984](#)). In the Samoa Islands, the tsunami reached 37 cm at Apia, and 2–2.5 m on Tutuila, according to newspaper reports compiled by [Pararas-Carayannis and Dong \(1980\)](#); however, this latter datum is not reported by [Solov'ev and Go \(1984\)](#). The times reported by [Solov'ev and Go \(1984\)](#) for arrival in Hawaii are again late, by at least five hours.

In summary, among the four large earthquakes of the late 1910s, Event II stands out as the major tsunamigenic source, and as such, as a predecessor to the 2009 earthquake. Its tsunami was demonstrably damaging in Samoa, but may however have remained smaller in amplitude than its 2009 counterpart.

In this context, during the international surveys conducted in the aftermath of the 2009 Samoa tsunami ([Richmond et al., 2009](#); [Okal et al., 2010](#)), we systematically asked witnesses on the islands of Upolu and Tutuila whether they had heard from their parents or grand-parents about the 1917 tsunami. We were motivated by our experience during previous post-tsunami surveys, where local

residents often described such ancestral heritage. For example, while interviewing elderly survivors of the 1946 Aleutian tsunami in the Marquesas, we met a witness whose grandfather had escaped a tsunami tentatively identified as the 1877 Chilean event ([Okal et al., 2002](#)). We anticipated that the tsunami from Event II, reported as causing major destruction and reaching 12-m run-up, would have remained vividly imprinted in the cultural heritage of the local populations.

Surprisingly, we found personal accounts of the 26 June 1917 tsunami to be extremely rare. Only two people from the same family, living on the South coast of Upolu, recalled their grandmother telling them that, when she was a child and living in Apia, she had run to high ground after feeling the earthquake and seeing the water recede ([J. and S. Annandale, pers. comm., 2009](#)). She had not given them any details about the wave height, because she had run inland and thus had not seen the wave(s) arriving. This report is intriguing given the contained height of the tsunami (90 cm peak-to-peak) and the polarity of the first arrival on the Apia maregram ([Fig. 8a](#)), but the location of the witness could be in doubt.

Furthermore, out of over one hundred tsunami survivors in (independent) Samoa, living in the areas affected by the 2009 tsunami and interviewed following the event by [Lani Wendt-Young](#), only four spoke of previous events, but none referred to the 1917 tsunami ([Wendt-Young, 2010](#)). One man remembered his elders talking about 'galu afi' (a wave of fire), which might possibly relate to the 1917 event, although no dates were provided ([L. Wendt-Young, pers. comm., 2010](#)). The only other personal account of the 1917 event is from an elderly Samoan lady from Savai'i. She was told by her mother-in-law, who was living in the Falealili District on the South coast of Upolu, that the tsunami struck just a year after (sic) the 'Faama'i oti' (disease of death, the flu epidemic); both had been traumatic experiences for her ([U. Hertel, pers. comm., 2010](#)).

Reports in the Samoa Times of 30 June 1917 suggest that the effects of the earthquake and tsunami were indeed much more severe and devastating on the south coast of Upolu and in the Aleipata region than near Apia ([Pararas-Carayannis and Dong, 1980](#)).

Asked whether the 1917 tsunami had been discussed at school, another witness replied that he remembered being told about the 1918 influenza epidemic, but not about the tsunami the previous year. The lack of recollection of the 1917 tsunami appears to be strongly linked with the 1918 influenza epidemic. The epidemic was caused when the disease was transferred by people onboard the ship *Talune* that arrived from New Zealand on 7 November 1918. According to Ministry of Health records in London, 7542 persons died in Samoa of the disease or related illnesses, out of a total population of 30,738, in rough numbers one Samoan in four ([James, 1920](#); [Boyd, 1980](#); [Tomkins, 1992](#)). Furthermore, the epidemic affected men and the elderly the hardest, with 30% of the male population dying of the disease, leading to the loss of 45% of the matai (head or titled members of an aiga (extended family group)) ([Tomkins, 1992](#)). Elderly men are the national keepers of tradition and history ([U. Hertel, pers. comm., 2009](#)), and their untimely death may have resulted in the loss of memory of previous events. Finally, the 1918 influenza epidemic had such a devastating effect on the population of Samoa that it is also likely that the effects of the 1917 tsunami, which did not appear to have resulted in any deaths despite extensive destruction in some villages on the south coast of Upolu ([Pararas-Carayannis and Dong, 1980](#)), were not retained in the memory of the survivors (of the tsunami and the influenza epidemic), as they had been overshadowed by the more tragic epidemic.

A further, and increasingly puzzling, aspect of this situation is that American Samoa was not affected by the influenza epidemic, as a result of a draconian quarantine of the entire territory ([Tomkins, 1992](#)). Yet, the memory of the 1917 tsunami is just as absent on Tutuila (where we could not obtain a single report of ancestral memory) as on Upolu, even though waves were reported in the 2 to 3-m range, churches were damaged in Pago Pago, and "natives around the bay sought refuge in the



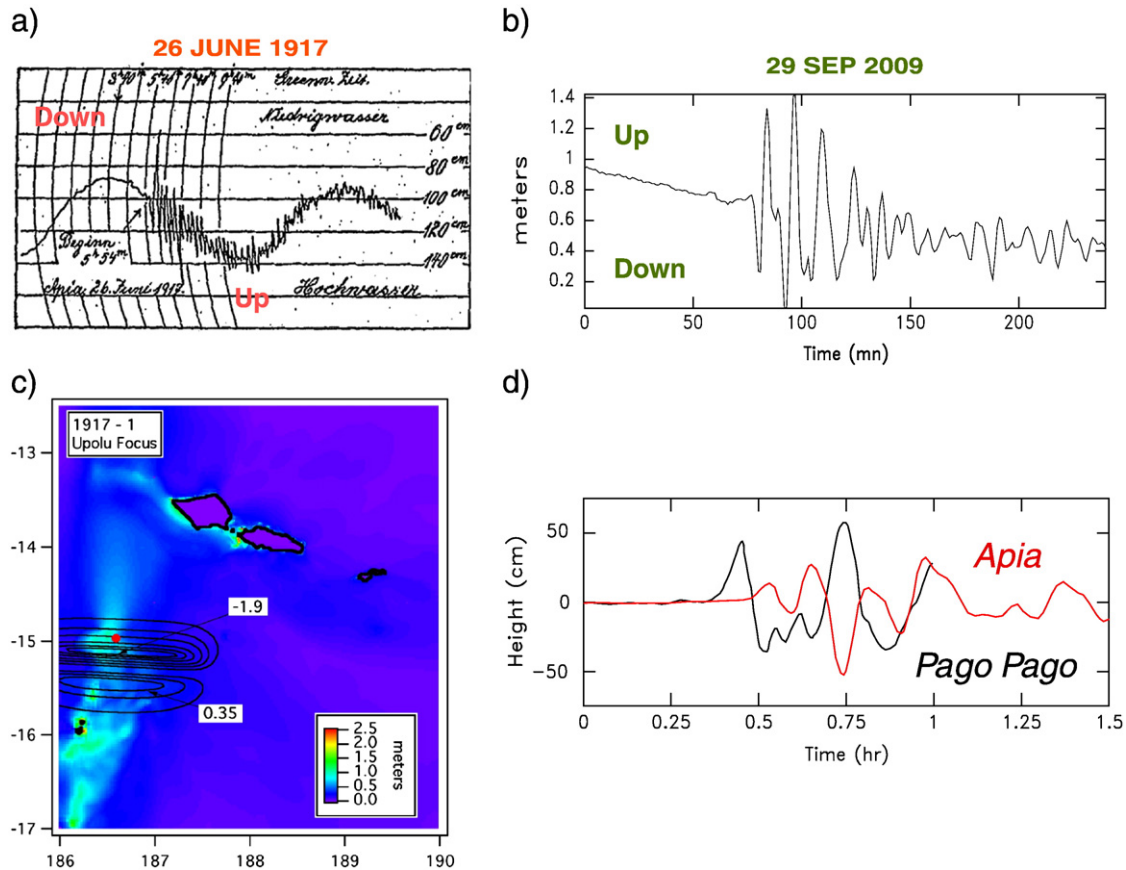


**Fig. 8.** (a) Tidal gauge record of Event II's tsunami at Apia, as published by Angenheister (1920). Note reversed vertical scale (“Hochwasser” [high water] downwards; “Niedrigwasser” [low water] upwards), indicating initial flooding. (b): Apia maregram of the 2009 tsunami. Note polarity opposite to 1917. (c): Field of deep-water amplitudes simulated for 1917 source. (d): Simulated maregrams at Pago Pago (black) and Apia (red).

mountains where they remained until morning” (O le Fa’atonu, quoted by Pararas-Carayannis and Dong, 1980).

Finally, no ancestral memories of previous large tsunamis were reported by the population of Niuatoputapu Island, Tonga, when interviewed during the survey of the 2009 Samoa tsunami, which reached its highest run-up (22 m) on nearby Tafahi (Okal et al., 2010).

### 6.2. Seismological study: Event I, 01 May 1917

We relocate this earthquake at 29.39°S, 179.29°W, approximately 100 km West of Raoul Island, and hence under the back-arc basin. However, its Monte Carlo ellipse ( $\sigma_C = 15$  s) intersects the subduction zone, in the vicinity of Gutenberg and Richter's (1954) and the ISS solutions.

The event is also close to the epicenter of the doublet of 14 January 1976. Those large events ( $6.0$  and  $8.2 \times 10^{27}$  dyn cm) featured thrust mechanisms on steeply dipping fault planes ( $\phi = 28^\circ$ ;  $\delta = 80^\circ$ ;  $\lambda = 93^\circ$  for the main (2nd) shock).

In addition to the Uppsala records used by Okal (1992a), we obtained Galitzin seismograms at De Bilt (DBN), on which we were able to verify an anaseismic PKP arrival compatible with a thrust mechanism (Fig. 9). We thus assume that Event I shares the above mechanism, and obtain corrected mantle magnitudes  $M_c = 8.37 \pm 0.20$  (Fig. 9).

Event I was followed on 16 November 1917 by a smaller shock ( $M_{PAS} = 7.5$ ), which we relocate 116 km to the NE, at 28.67°S, 178.42°W; the relative location of the two events being reminiscent of that of the 1976 doublet. Solov'ev and Go (1984) mention local tsunami waves in Tonga, but not elsewhere.

### 6.3. Seismological study: Event II, 26 June 1917

We relocate this earthquake at 15.13°S, 173.28°W (Fig. 1), a solution just 50 km NW of Gutenberg and Richter's (1954), but more than 260 km away from the ISS epicenter which falls outside the Monte Carlo confidence ellipse (computed with  $\sigma_C = 15$  s). Our epicenter is also less than 30 km from that of the 1981 event. Thus the 1917 earthquake falls within the general cluster of seismicity expressing the STEP (Govers and Wortel, 2005) along the Samoan elbow of the Tongan plate boundary. The 2009 epicenter plots on the fringe of the 1917 confidence ellipse, and it is unlikely that the two events represent a common process at the same location.

In addition to the Uppsala records used by Okal (1992a), we obtained seismograms at De Bilt (DBN) and Strasbourg (STR). These stations do not provide enough azimuthal coverage to allow a PDFM solution of the moment tensor (Reymond and Okal, 2000), and thus the focal geometry of the event cannot be inverted. In this context, the North–South Wiechert record at STR is crucial (Fig. 10), since it shows a strong impulsive PKP arrival to the South (we have verified (L. Rivera, pers. comm., 2010) that the polarity of this component was inverted, with an upwards motion corresponding to Southwards ground motion). With a back-azimuth  $\beta = 1.8^\circ$ , this represents an anaseismic first motion, which in itself rules out a mechanism similar to the one in 1981. We note that the largest CMT solutions in the vicinity of the epicenter feature a wide variety of focal mechanisms, and thus the mechanism of the 1917 event remains otherwise unresolved. The thrusting character of Event II is also supported by the examination of the Apia maregram, reproduced on Fig. 8a from Angenheister (1920), which clearly shows an initial flooding (note the inverted scale), as opposed to an initial down-draw in 2009 (Fig. 8b).

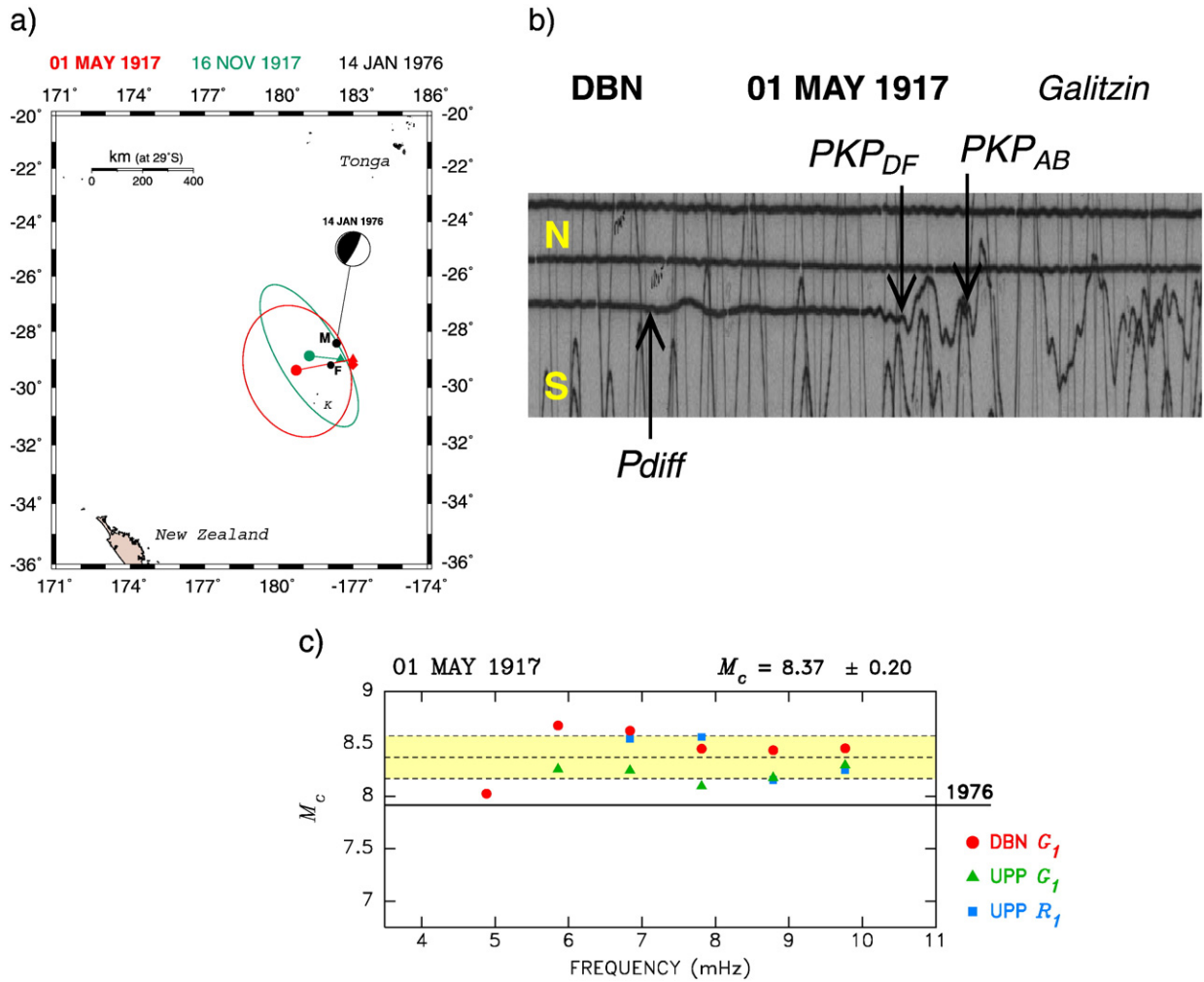


**Fig. 9.** (a): Relocation of Event I (01 May 1917) in the Kermadec Islands (K). The red dot is the relocated epicenter with its Monte Carlo ellipse; also shown are Gutenberg and Richter's (1954) solution (red triangle) and the ISS location (diamond). The relocation of the aftershock of 16 November 1917 is shown in green. The two black dots show the epicenters of the 1976 doublet (M, main shock, with mechanism; F, foreshock). (b): Close-up of the North-South Galitzin record of Event I at De Bilt. Note the PKP phases, impulsive to the South, as well as Pdiff, tentatively emergent to the South. These observations establish anaseismic first motions, compatible with a thrust mechanism. The vertical coordinate on this record was amplified 2.5 times, to enhance impulsive arrivals. The record is 5 mn 9 s long. (c): Estimation of seismic moment from spectral amplitudes and mantle magnitudes  $M_c$  corrected for the 1976 focal mechanism. The moment of the latter event is shown as the solid line.

In the absence of a reliable focal mechanism, the moment of the event can be estimated from its mantle magnitudes  $M_m$ , uncorrected for focal geometry. An average taken between periods of 100 and 250 s yields  $M_m = 7.94 \pm 0.34$  (Fig. 10). These results confirm that the 1917 event is comparable to, if probably somewhat smaller than, the 2009 earthquake.

Noting the increase of magnitudes at long periods, and for the purpose of carrying out realistic simulations of the 1917 tsunami, we use a moment  $M_0 = 1.2 \times 10^{28}$  dyn cm, and a mechanism inspired by the nearby earthquakes of 16 May 1993 and 07 April 1995:  $\phi = 288^\circ$ ;  $\delta = 75^\circ$ ;  $\lambda = 67^\circ$ . The results of our simulations are shown on Fig. 8c and d. Note that they reproduce the main characteristics of the maregram published by Angenheister (1920), namely a positive first wave and a peak-to-peak amplitude on the order of 90 cm (Fig. 8a).

#### 6.4. Seismological study: Event III, 01 January 1919

Using 13 travel times listed in the ISS, we obtain a preferred hypocenter at  $19.52^\circ\text{S}$ ,  $177.61^\circ\text{W}$  and 246 km depth. This depth is in reasonable agreement with Gutenberg and Richter's (1954) solution (180 km), but would place the event more than 200 km above the

local Benioff zone. When running Wyssession et al.'s (1991) Monte Carlo algorithm (with  $\sigma_c = 10$  s), we find epicenters reaching the 200-km deep portion of the slab, and also inverted depths ranging from 3 to 540 km, indicating poor control on source depth. However, the Monte Carlo ellipse does not reach the region of shallow seismicity expressing interplate thrust (Fig. 7). Thus, Event III is most probably of intermediate depth, in the 150 to 250 km range, as further suggested by Engdahl and Villaseñor's (2002) relocation at  $19.97^\circ\text{S}$ ,  $177.91^\circ\text{W}$  and 203 km. In Okal (1992b), we had proposed a moment of  $6.3 \times 10^{27}$  dyn cm, based on Rayleigh spectral amplitudes at Uppsala, and assuming the same focal mechanism as that of the large intermediate depth event of 22 May 1972 ( $\phi = 55^\circ$ ;  $\delta = 60^\circ$ ;  $\lambda = -118^\circ$ ), as studied by Denham (1977). The combination of this moment and the depth of the event rule out the generation of a tsunami observable in Japan, thus supporting Iida et al.'s (1967) claim of an erroneous association. In this context, and in the absence of local tsunami reports, no hydrodynamic simulation seems warranted.

#### 6.5. Seismological study: Event IV, 30 April 1919

We relocate this event to  $18.49^\circ\text{S}$ ,  $173.36^\circ\text{W}$ , which is significantly West of the subduction zone. However, the Monte Carlo

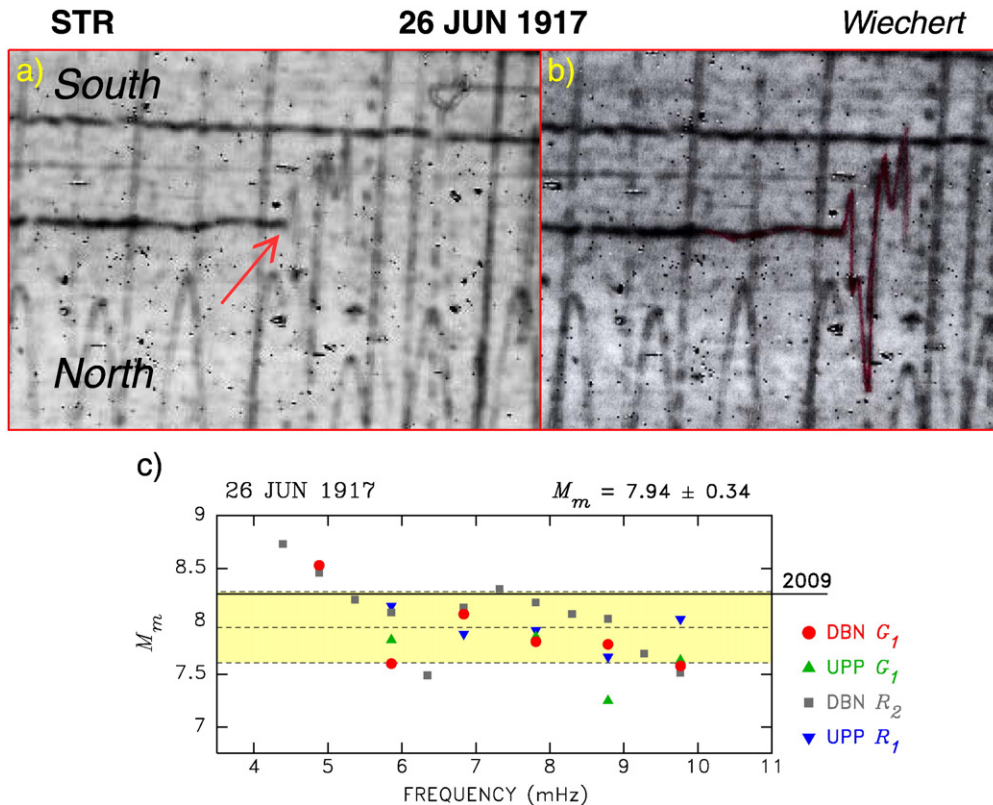


**Fig. 10.** (a): Close-up of the PKP arrival (arrow) at Strasbourg ( $\Delta = 147^\circ$ ), as recorded on the NS component of the Wiechert seismometer. In (b), we have traced the waveform to illustrate the upwards polarity of the arrival. The combination of a reversed polarity of the instrument (Southward ground motion to the top), and of a back-azimuth of  $1.8^\circ$  makes this an anaseismic arrival, requiring a thrust component in the focal mechanism. (c): Mantle magnitudes computed for Event II at De Bilt and Uppsala. The dashed line and shaded area represent the average value of  $M_m$  and confidence interval. The solid line shows the moment of the 2009 event, for comparison. Note possible increase of 1917 moment at lowest frequencies.

ellipse ( $\sigma_C = 15$  s) intersects it, and includes [Gutenberg and Richter's \(1954\)](#) solution ([Fig. 1](#)). The ISS solution, farther South and in the outer rise, can be excluded. The relocation has no depth resolution and there is no reason to assume that the source is not shallow. In addition to the Uppsala records studied in [Okal \(1992a\)](#), we obtained a single component of the Hongo (Tokyo) NS record, featuring a prominent  $G_1$  arrival. The records at De Bilt could not be used as the recording chart was being changed at the time of arrival of the main mantle waves. This dataset is insufficient to conduct a PDFM inversion ([Reymond and Okal, 2000](#)), and the mechanism can only be speculated. We note that the largest local CMT solutions (e.g., 06 October 1987;  $M_0 = 8.9 \times 10^{26}$  dyn cm) feature normal faulting, which is supported by a kataseismic  $P$  arrival on the available Hongo record ([Fig. 11](#)). Assuming a geometry similar to the 1987 earthquake ( $\phi = 352^\circ$ ,  $\delta = 42^\circ$ ,  $\lambda = -113^\circ$ ), we compile on [Fig. 11](#) corrected mantle magnitudes of average value  $M_c = 8.06 \pm 0.38$ , suggesting that Event IV is comparable in size (and presumably in mechanism) to the 1977 earthquake farther South ([Fig. 1](#)), but smaller than the 2009 event.

## 7. Other notable events

In addition to the events studied above, the following earthquakes generated tsunamis recorded with decimetric amplitudes in Samoa: 06 October 1987 ( $18.29^\circ\text{S}$ ,  $171.93^\circ\text{W}$ ;  $M_0 = 8.9 \times 10^{26}$  dyn cm), 22 June 1977 ( $22.86^\circ\text{S}$ ,  $174.91^\circ\text{W}$ ;  $M_0 = 1.4 \times 10^{28}$  dyn cm), and 03 May 2006 ( $20.39^\circ\text{S}$ ,  $173.47^\circ\text{W}$ ;  $M_0 = 1.1 \times 10^{28}$  dyn cm). Note that none of them expresses subduction at the Tonga trench. These events are shown as squares on [Fig. 1](#). A number of additional earthquakes generated tsunamis, which were recorded at centimetric amplitudes in Samoa ([Pararas-Carayannis and Dong, 1980](#); [Solov'ev and Go, 1984](#)).

Finally, [Okal et al. \(2004\)](#) modeled the Tongan event of 17 November 1865, which generated the only tsunami from the Kermadec–Tonga–Samoa province recorded in the far field at directly observable amplitudes (as opposed to instrumentally). They showed that it required a seismic moment of  $4 \times 10^{28}$  dyn cm, significantly larger than instrumentally measured in the past 100 years, and in particular than those of the 2009 earthquake and of Events I–IV. They could not, however, resolve the geometry of the 1865 earthquake as interplate thrust, intraplate slab break, or outer rise normal faulting. Nevertheless, there remains the important conclusion that tsunami hazard from the arc, especially in the far field, is definitely undersampled by the window of historical seismicity.

On [Fig. 1](#), we also show as inverted triangles historical events of the Samoa corner (i.e., with an initial latitude North of  $20^\circ\text{S}$ ), with at least one reported magnitude  $M \geq 7$ , but without reported tsunamis. We relocated these earthquakes as part of this study, and their parameters are listed in [Table 1](#).

## 8. Conclusion

We have examined the principal historical earthquakes which generated tsunamis in the Samoa Islands in the past hundred years. The more recent and smaller events of 1975 and 1981 are well constrained, and the effects of their tsunamis can be modeled successfully.

The most remarkable earthquakes are the series of three large events (II, III, and IV) having occurred in Samoa–Tonga in 1917–1919, to which we add the more distant Kermadec earthquake (Event I). Of those, it is clear that only Event II (26 June 1917) generated a destructive tsunami in Samoa, and thus can be considered a predecessor to the 2009 earthquake. We obtain a moment estimate of  $1.2 \times 10^{28}$  dyn cm, slightly lower than for 2009. On the other hand,

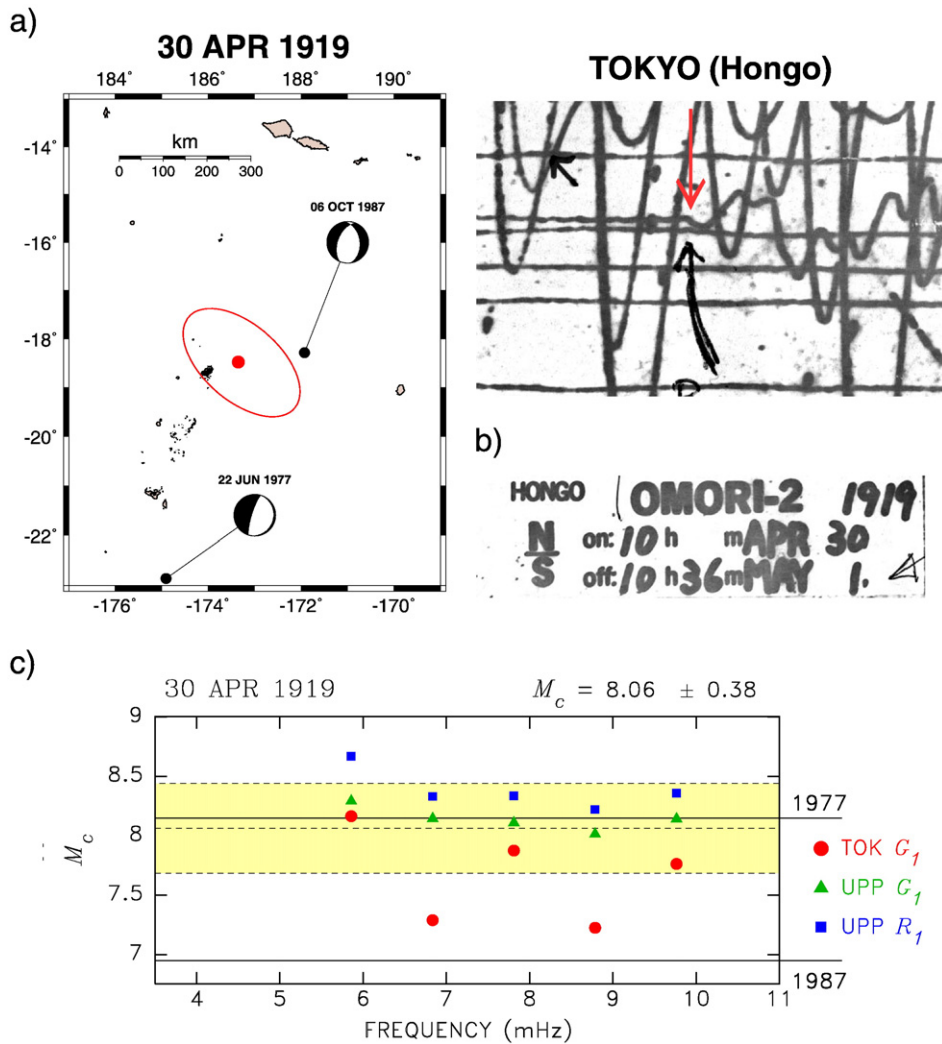


**Fig. 11.** (a): Relocation of Event IV (30 April 1919). The red dot is the relocated epicenter with its Monte Carlo ellipse; also shown is the nearby normal faulting event of 06 October 1987 whose mechanism we assume, as well as the large normal faulting 1977 earthquake in Tonga to the South. (b): Close-up of the P arrival (arrow) on the North–South Omori-2 record at Tokyo (Hongo). The station stamp (also shown) proves a Southward first motion, which results in a kataseismic polarity requiring a component of normal faulting. (c): Estimation of seismic moment from mantle magnitudes  $M_c$ , corrected for the 1987 mechanism, and comparison with the moments of the 1977 and 1987 events.

and while Event I is probably the larger of the four, the claim of a 12-m wave in Samoa is unrealistic due to distance, and most probably the result of confusion with Event II, just 56 days later.

In contrast to our experience in several other areas regularly affected by tsunamis, our interviews during field surveys indicate, with a few rare exceptions, a lack of ancestral memory of the 1917 event among the present residents of Samoa. We tentatively attribute this intriguing result to the 1918 influenza epidemic, which was a much more severe disaster and contributed to eradicate the means of ancestral transmission to the present generations.

A most remarkable aspect of Event II is that it occurs in the immediate vicinity of the 1981 earthquake but cannot share its focal mechanism, based on critical polarity data recorded at Strasbourg and on the Apia maregraph. While a large diversity of focal mechanisms is indeed documented in that complex region in the CMT catalogue, our study shows that it also characterizes the largest shocks. This means that the next Samoa earthquake to cause a destructive tsunami has an unpredictable geometry, and in particular that its tsunami could feature a leading inundation at the local beaches. This was the case during Event II as documented by the Apia maregram (Fig. 7a), and would deprive the population of the natural element of safe warning provided by a leading depression.

Finally, we note that none of the Samoa tsunamigenic earthquakes studied had an interplate thrust mechanism expressing the subduction of the Pacific plate at the Tonga Trench. While the existence of such events may not be totally ruled out, this result supports the model of a mostly aseismic subduction at this boundary, characterized by a high lithospheric age and exceptionally fast convergence (Bevis et al., 1995).

**Acknowledgments**

We thank Sose and Joe Annandale, and Ulrike Hertel for providing unique accounts about the 1917 Samoa tsunami, as well as Lani Wendt-Young for her help. We are grateful to Jim Dewey, Harley Benz, Steve Kirby, Bernard Dost and Luis Rivera for access to the seismological archives in Golden, De Bilt and Strasbourg. The paper was improved by the comments of Hermann Fritz and an anonymous reviewer. Maps were drawn using the GMT software (Wessel and Smith, 1991).

**References**

Angenheister, G., 1920. Vier Erdbeben und Flutwellen im Pazifischen Ozean, beobachtet am Samoa-Observatorium, 1917–1919. Nachr. K. Gesellsch. Wissensch. Göttingen 201–204.



- Bevis, M., Taylor, F.W., Chutz, B.E., Recy, J., Isacks, B.L., Helu, S., Singh, R., Kendrick, E., Stowell, J., Taylor, B., Calmant, S., 1995. Geodetic observations of very rapid convergence and back-arc extension at the Tonga arc. *Nature* 374, 249–251.
- Boyd, M., 1980. Coping with Samoan resistance after the 1918 influenza epidemic. *J. Pac. Hist.* 15, 155–174.
- Denham, D., 1977. Summary of earthquake focal mechanisms for the Western Pacific–Indonesian region, 1929–1973. U.S. Dept. of Commerce, World Data Center A, Boulder. Rept. SE-3, 110 pp.
- Dziewonski, A.M., Chou, A.-T., Woodhouse, J.H., 1981. Determination of earthquake source parameters from waveform data for studies of global and regional seismicity. *J. Geophys. Res.* 86, 2825–2852.
- Dziewonski, A.M., Ekström, G., Franzen, J.E., Woodhouse, J.H., 1988. Global seismicity of 1981; Centroid moment tensor solutions for 542 earthquakes. *Phys. Earth Planet. Inter.* 50, 155–182.
- Engdahl, E.R., Villaseñor, A., 2002. Global seismicity: 1900–1999. In: Lee, W.H.K., Kanamori, H., Jennings, P.C., Kisslinger, C. (Eds.), *International Handbook of Earthquake and Engineering Seismology, Part A, Chapter 41*. Academic Press, pp. 665–690.
- Geller, R.J., 1976. Scaling relations for earthquake source parameters and magnitudes. *Bull. Seismol. Soc. Am.* 66, 1501–1523.
- Govers, R., Wortel, M.J.R., 2005. Lithosphere tearing at STEP faults: response to edges of subduction zones. *Earth Planet. Sci. Lett.* 236, 505–523.
- Gutenberg, B., Richter, C.F., 1954. *Seismicity of the Earth and Associated Phenomena*. Princeton Univ. Press, 310 pp.
- Heck, N.H., 1947. List of seismic sea waves. *Bull. Seismol. Soc. Am.* 37, 269–286.
- Iida, K., Cox, D.C., Pararas-Carayannis, G., 1967. Preliminary catalog of tsunamis occurring in the Pacific Ocean. Data Rep. 5 Hawaii Inst. Geophys., Honolulu. HIG-67-10, 275 + 27 pp.
- Imamura, A., Moriya, M., 1939. Maregraphic observations of tsunamis in Japan during the period from 1894 to 1924. *Jpn J. Astron. Geophys.* 17, 119–140.
- James, S.P., 1920. The general statistics of influenza in Australasia and parts of Africa and Asia. Reports on public health and medical subjects. No. 4. Report on the pandemic of influenza, 1918–19, Chapter II. H.M.'s Stationery Office, London, pp. 349–386 [http://influenza.sph.unimelb.edu.au/MOH\\_TOC.php](http://influenza.sph.unimelb.edu.au/MOH_TOC.php) (accessed 24 June 2010).
- Kagan, Y.Y., 1991. 3-D rotation of double-couple earthquake sources. *Geophys. J. Intl.* 106, 709–716.
- Kirby, S.H., Hino, R., Umino, N., Gamage, S., Hasegawa, A., Engdahl, E.R., Bergman, E., 2008. The 75th anniversary of the great Sanriku-oki, Japan earthquake of March 2nd, 1933: new observations and new insights into the largest recorded outer-rise earthquake. *EOS Trans. Am. Geophys. Union* 89 (53), S14A-05 [abstract].
- Lay, T., Ammon, C.J., Kanamori, H., Rivera, L., Koper, K.D., Hutko, A.R., 2010. The Samoa–Tonga great earthquake triggered doublet. *Nature* 466, 964–968.
- Li, X., Shao, G., Ji, C., 2009. Rupture process of  $M_w = 8.1$  Samoa earthquake constrained by joint inverting teleseismic body, surface waves and local strong motion. *EOS Trans. Am. Geophys. Union* 90 (53), U21D-03 [abstract].
- Lundgren, P.R., Okal, E.A., 1988. Slab decoupling in the Tonga arc: the June 22, 1977 earthquake. *J. Geophys. Res.* 93, 13355–13366.
- Okal, E.A., 1992a. Use of the mantle magnitude  $M_m$  for the reassessment of the seismic moment of historical earthquakes. I: shallow events. *Pure Appl. Geophys.* 139, 17–57.
- Okal, E.A., 1992b. Use of the mantle magnitude  $M_m$  for the reassessment of the seismic moment of historical earthquakes. II. Intermediate and deep events. *Pure Appl. Geophys.* 139, 59–85.
- Okal, E.A., Talandier, J., 1989.  $M_m$ : a variable period mantle magnitude. *J. Geophys. Res.* 94, 4169–4193.
- Okal, E.A., Synolakis, C.E., Fryer, G.J., Heinrich, P., Borrero, J.C., Ruscher, C., Arcas, D., Guille, G., Rousseau, D., 2002. A field survey of the 1946 Aleutian tsunami in the far field. *Seismol. Res. Lett.* 73, 490–503.
- Okal, E.A., Borrero, J.C., Synolakis, C.E., 2004. The earthquake and tsunami of 17 November 1865: evidence for far-field tsunami hazard from Tonga. *Geophys. J. Intl.* 157, 164–174.
- Okal, E.A., Sladen, A., Okal, E.A.-S., 2006a. Rodrigues, Mauritius and Réunion Islands field survey after the December 2004 Indian Ocean tsunami. *Earthquake Spectra* 22, S241–S261.
- Okal, E.A., Fritz, H.M., Raveloson, R., Joelson, G., Pančoškova, P., Rambolamanana, G., 2006b. Madagascar field survey after the December 2004 Indian Ocean tsunami. *Earthquake Spectra* 22, S263–S283.
- Okal, E.A., Fritz, H.M., Sladen, A., 2009. 2004 Sumatra tsunami surveys in the Comoro Islands and Tanzania and regional tsunami hazard from future Sumatra events. *S. Afr. J. Geol.* 112, 343–358.
- Okal, E.A., Fritz, H.M., Synolakis, C.E., Borrero, J.C., Weiss, R., Lynett, P.J., Titov, V.V., Foteinis, S., Jaffe, B.E., Liu, P.L.-F., Chan, I., 2010. Field survey of the Samoa Tsunami of 29 September 2009. *Seismol. Res. Lett.* 81, 577–591.
- Pararas-Carayannis, G., Dong, B., 1980. Catalog of tsunamis in the Samoan Islands. Intl. Tsunami Infor. Center, Honolulu. 75 pp.
- Reymond, D., Okal, E.A., 2000. Preliminary determination of focal mechanisms from the inversion of spectral amplitudes of mantle waves. *Phys. Earth Planet. Inter.* 121, 249–271.
- Reymond, D., Hyvernaud, O., Hébert, H., Okal, E.A., Jamelot, A., Allgeyer, S., 2010. Field survey and preliminary simulation of the 2010 Maule, Chile, tsunami in French Polynesia. *Seismol. Res. Lett.* 81 Ann. Meeting Prog., p. 37, [abstract].
- Richmond, B.M., Buckley, M.L., Etienne, S., Strotz, L.C., Chagué-Goff, C., Wilson, K., Goff, J.R., Dudley, W.C., Sale, F., 2009. Geologic signatures of the September 2009 South Pacific tsunami. *Eos Trans. Am. Geophys. Union* 90 (52), U24A-05 [abstract].
- Solov'ev, S.L., Go, T.ch.N., 1975. Katalog tsunami na vostochnom poberezh'e tikhovo okeana. 204 pp. Akad. Nauk SSSR, Moskva. [in Russian].
- Solov'ev, S.L., Go, Ch.N., 1984. Catalogue of tsunamis on the Eastern shore of the Pacific Ocean. *Can. Transl. Fish. Aquat. Sci.* 5078, 293 pp.
- Solov'ev, S.L., Go, T.ch.N., Kim, Kh.S., 1986. Katalog tsunami v tikhom okeane, 1969–1982 gg. Akad. Nauk SSSR, Moskva. 164 pp.
- Talandier, J., Okal, E.A., 1979. Human perception of  $T$  waves: the June 22, 1977 Tonga earthquake felt on Tahiti. *Bull. Seismol. Soc. Am.* 69, 1475–1486.
- Titov, V.V., Synolakis, C.E., 1998. Numerical modeling of tidal wave runup. *J. Waterw. Port Coast. Ocean Eng.* B124, 157–171.
- Tomkins, S.M., 1992. The influenza epidemic of 1918–19 in Western Samoa. *J. Pac. Hist.* 27, 181–197.
- Wendt-Young, L., 2010. Stories of the 'Galufi'. Samoa Observer, Apia. 14 February.
- Wessel, P., Smith, W.H.F., 1991. Free software helps map and display data. *EOS Trans. Am. Geophys. Union* 72, 441 and 445–446.
- Wyssession, M.E., Okal, E.A., Miller, K.L., 1991. Intraplate seismicity of the Pacific Basin, 1913–1988. *Pure Appl. Geophys.* 135, 261–359.